ACS NANO

www.acsnano.org

ARTICLE

Gyroscope-Structured Triboelectric Nanogenerator for Harvesting Multidirectional Ocean Wave Energy

Qi Gao,[⊥] Yuhong Xu,[⊥] Xin Yu, Zhaoxu Jing, Tinghai Cheng,* and Zhong Lin Wang*

Cite This: https://doi.org/10.1021/acsnano.2c01594

Read Online

ACCESS | Metrics & More | Article Recommendations | Supporting Information

ABSTRACT: **Wave motion in the ocean can generate plentiful energy, but it is difficult to harvest wave energy for practical use because of the low frequency and random directional characteristics of wave motion. In this paper, a gyroscope-structured triboelectric nanogenerator (GS-TENG) is proposed for harvesting multidirectional ocean wave energy. Its inner and outer generation units can operate independently in different directions, and they all adopt the friction mode of surface contact. While realizing noninterference multidirectional energy harvesting, the power generation area is increased. In the experiments, under acceleration of 6 m/s^2 with variations in excitation angle, the GS-TENG can output direct currents of 0.8−3.2 μA, and the open-circuit voltages of the inner and outer generation units can reach 730 and 160 V, respectively. When the devices are networked and placed in the water, the electrical energy generated by the GS-TENGs can enable commercial thermometers to operate normally. The attenuation of direct-current output by the GS-TENG in the experiment of 30 days in water is about 8%, which verifies the good durability of the device in the water environment. Therefore, the GS-TENG has excellent application prospects in the wave energy harvesting field.**

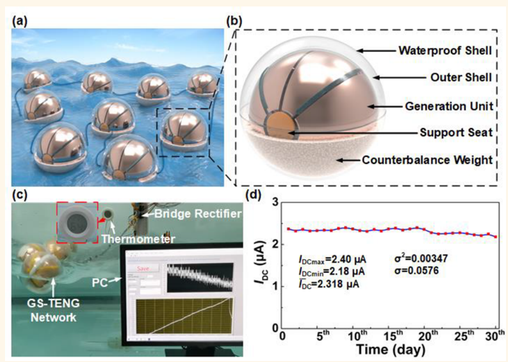

KEYWORDS: *triboelectric nanogenerator, ocean wave, multidirectional energy harvesting, gyroscope structure, surface contact*

INTRODUCTION

As the energy crisis continues to grow, active development of renewable energy sources and continuous improvement in the utilization rate of these sources represent the inevitable choices that must be made to solve the current energy problems.[1−3] At present, because of its large and high-density energy reserves, the ocean has become the renewable energy source with the greatest potential for commercial development. Wave energy is the richest and most widely distributed energy source in the ocean, which means that increased development of wave energy technology will be conducive to the sustainable development of the ocean's natural resources.[4,5] However, in their natural environment, waves have characteristics that include low fluctuation frequencies (generally less than 5 Hz) and strongly random fluctuation states. Therefore, it will be vital to develop a technology that can harvest wave energy effectively.

In 2012, Wang's group first proposed the triboelectric nanogenerator (TENG), which attracted the attention of researchers worldwide because it can convert mechanical energy from nature into output electrical energy.[6−8] TENGs have characteristics that include small size,[9,10] low cost,[11,12] and ease of manufacturing,[13,14] and they are particularly useful in harvesting of low-frequency mechanical energy with high efficiency.[15−17] Therefore, TENGs are widely used in fields such as micronano energy harvesting,[18−21] self-driven sensing,[22−25] and high voltage power supplies.[26−28] In particular, TENGs offer numerous advantages for applications in the harvesting of ocean energy, which is known as blue energy.[29−31] Additionally, if multiple TENG units are integrated into a network structure to enable large-scale wave energy harvesting in the ocean, they can provide a technological approach to harness a wide range of blue energy sources.[32−34] Since the TENG was first proposed, researchers in various countries have designed multiple types of TENG for wave energy harvesting.[35−37] However, due to the random nature of the direction of waves, there is a certain bottleneck in the multidirectional harvesting technology of ocean energy. Most of the harvesting schemes use the ball-sleeve or multi-ball structure.[38,39] Although

Received: February 15, 2022
Accepted: March 28, 2022

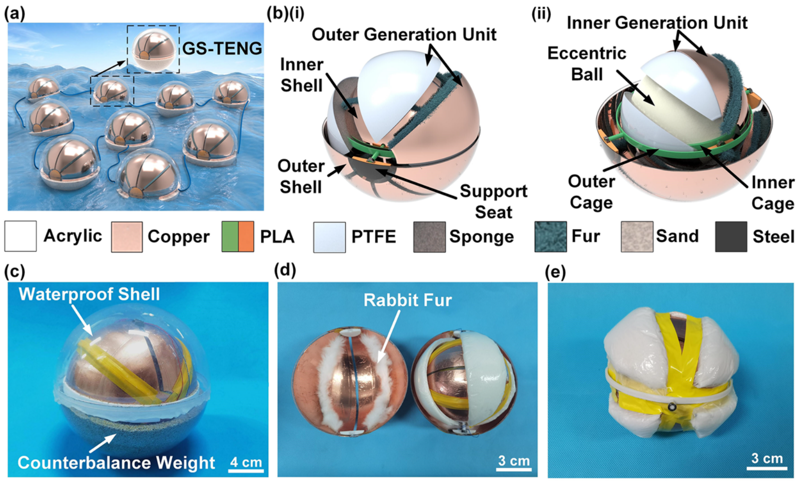

Figure 1. Structural design of gyroscope-structured triboelectric nanogenerator for harvesting multidirectional ocean energy (GS-TENG): (a) large-scale offshore energy harvesting network constructed using multiple GS-TENGs; (b) internal structural details; (c)−(e) photographs of prototypes.

multidirectional harvesting can be realized, the real-time contact area of the generation unit is small. Therefore, it is necessary to develop a TENG with a large power generation area and effective harvesting of multidirectional wave energy.

On the basis of the issues described above, this work proposes a gyroscope-structured triboelectric nanogenerator (GS-TENG) for multidirectional ocean wave energy harvesting. Inner and outer generation units with identical electrode arrangements are installed in the GS-TENG structure by using two cages with mutually perpendicular central axes. Since the two generation units are overhead by cages, the friction material can be in surface contact to increase the power generation area. When the GS-TENG is excited by water waves in random directions, the action of the cages allows the two generation units to move freely and independently in different directions and convert mechanical energy from the waves into electrical energy for output. The output performance of the proposed GS-TENG is tested by using linear motors to simulate wave motions with various accelerations and directions. When the acceleration reaches 6 m/s^2 and the excitation direction is varied, the open-circuit voltage output by the inner generation unit of the GS-TENG can reach 730 V, while that from the outer generation unit can reach 160 V; the direct current realized after rectification and parallel output can reach 0.8−3.2 μA, the peak power of the GS-TENG is 0.6 mW, and the peak power density is 0.28 W/m^3. Further application tests performed in a real-wave environment verify that a single GS-TENG can illuminate a light-emitting diode (LED) board continuously. Multiple GS-TENGs can be connected in an orderly network to realize large-scale wave energy harvesting, and the electrical energy output by such a network can drive a commercial thermometer to allow it to operate normally. The output performance of the GS-TENG remained stable throughout a 1 month long water experiment, thus proving its reliability. This research provides a concept for the structural design of TENGs for ocean wave energy harvesting.

RESULTS AND DISCUSSION

Structure and Working Principle. Wave energy is widely distributed in the marine environment and is a type of blue energy that offers significant economic benefits; this means that it is highly important to develop and use this energy source effectively. To enable effective multidirectional wave energy harvesting, the GS-TENG is designed as shown in Figure 1. First, the expected application of the gyroscope-structured triboelectric nanogenerator (GS-TENG) is described (see Figure 1a). Large-scale harvesting of random wave energy in the ocean can be enabled by networking of the GS-TENG, and such networks can act as distributed power supplies for electrical equipment. The internal structure model of the GS-TENG is illustrated clearly in Figure 1b; the model mainly includes an eccentric ball, inner and outer generation units, inner and outer shells, inner and outer cages, and support seats. The eccentric ball is connected to the inner shell through the inner cage and the support seat. In addition, the inner shell is connected to the outer shell through the outer cage and the support seat, and the central axes of the two cages are oriented perpendicular to each other.

The inner generation unit consists of sponge blocks covered with polytetrafluoroethylene (PTFE) that are located on the surface of the eccentric ball, and an inner shell with copper electrodes on its inner wall. Considering the interval area waste caused by too many electrodes and the small current caused by too few electrodes, the number of copper electrodes is set to eight, so there are four sponges with PTFE. To reduce the wear between materials, a specific gap is maintained between the PTFE and the copper electrodes, and four rabbit fur strips are distributed evenly on the inner wall of the inner shell to improve the charge density on the PTFE surface.[40] To show the detailed structure of the inner generation unit more clearly, please refer to Figure S1 (Supporting Information). The outer generation unit has a similar structure to the inner unit, with the exception of the PTFE and the copper electrodes being distributed evenly on the outer wall of the inner shell and the inner wall of the outer shell, respectively. Two generation units are overhead by cages, which will produce a certain interval, so the friction material and copper electrode can keep surface contact during operation, which increases the real-time power generation area. In addition, to avoid any interference being caused by the water when the GS-TENG is operational, the device is placed in a waterproof shell with good sealing performance, and the counterbalance weight is filled to enhance its ability to withstand the water wave force (Figure 1c). Figure 1 panels d and e show the physical structure in greater detail.

https://doi.org/10.1021/acsnano.2c01594
ACS Nano XXXX, XXX, XXX−XXX

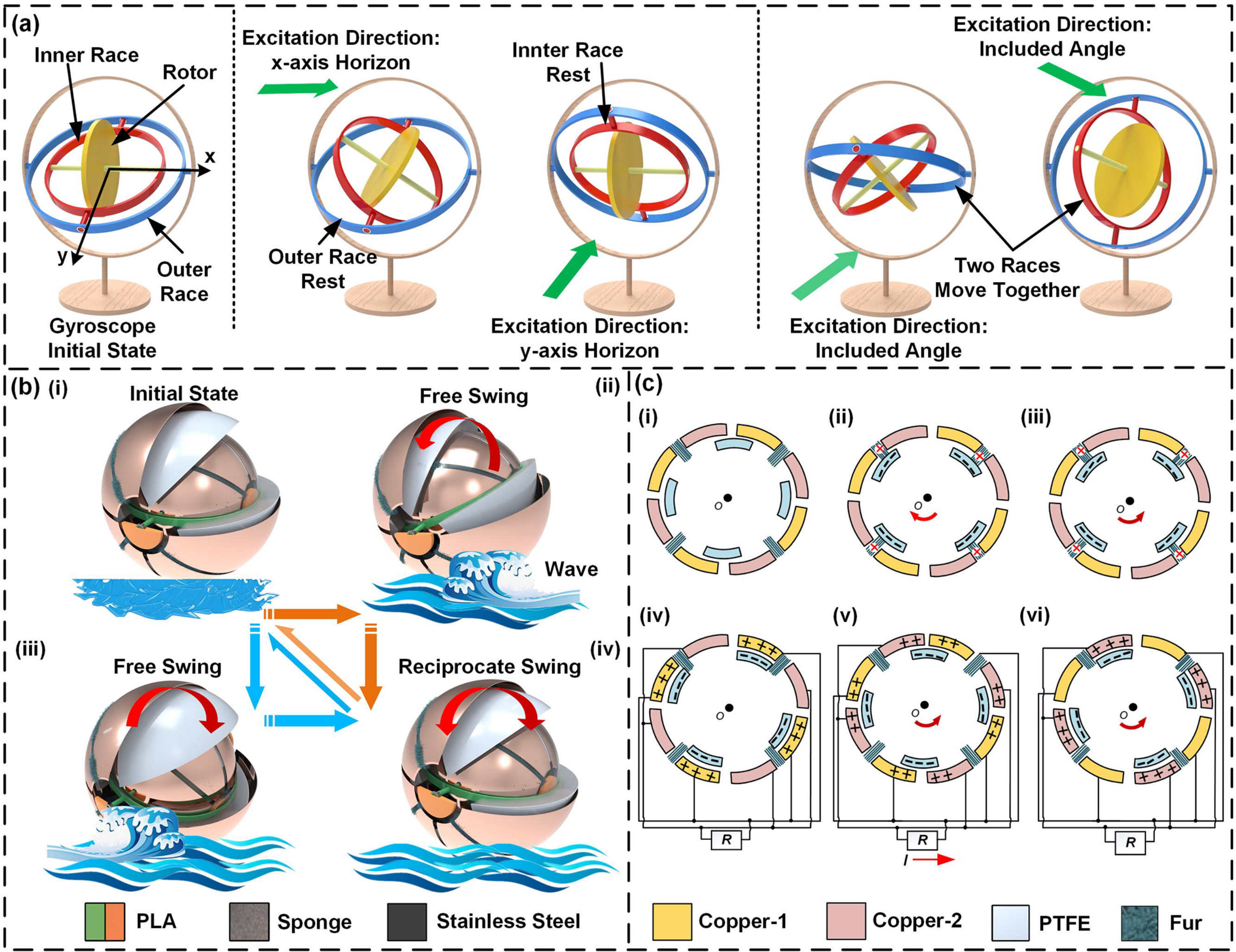

Figure 2. Schematic diagram of the working principle of the GS-TENG: (a) operational modes of the gyroscope; (b) operating mechanism of the GS-TENG under excitement from different directions; (c) device power generation principles.

The GS-TENG is designed on the basis of a gyroscope and is mainly composed of a rotor, an inner race, and an outer race; its operating mode is illustrated in Figure 2a. The central axis of the outer race is set as the x-axis, and the central axis of the inner race is set as the y-axis. Only the inner race can rotate when the direction of excitation is horizontal to the x-axis, and the outer race is at rest in this case. In contrast, when the direction of excitation is horizontal to the y-axis, the inner race remains at rest. Application of a stimulus from any direction other than these two specific directions will cause the two races to operate simultaneously.

The operating mode of the inner and outer cages, which are oriented perpendicular to each other in the GS-TENG, is the same as that for the inner and outer races of the gyroscope mechanism. When wave excitation from any direction acts on the device, the GS-TENG is driven by the wave force and begins to swing freely; then, when the wave excitation subsequently disappears, the swing reciprocates because of the inertia of the eccentric ball (Figure 2b). Throughout the entire process, because of the randomness of the direction of excitation, the two cages in the GS-TENG will alternately rotate either independently or jointly, thus driving the eccentric ball and the inner shell to swing and allowing the inner and outer generation units to operate independently without interfering with each other. Therefore, the GS-TENG can harvest multidirectional wave energy and output electrical energy continuously. The specific movement details of the inner generation unit under excitation are shown in Figure S2 (Supporting Information).

Figure 2c illustrates the power generation principles of the GS-TENG. When the GS-TENG swings under the application of external excitation, the PTFE film in the generation unit is charged via contact with the rabbit fur [Figure 2c(i)−(iii)]. In addition, Figure 2c images iv−vi show additional power generation principles of the GS-TENG. According to the triboelectric sequence, it is much easier for the PTFE to gather electrons than copper.[41] Therefore, because of the principle of electrostatic induction, the copper-1 component has a positive charge, and the PTFE film above it has an equal negative charge [Figure 2c-(iv)]. After excitation, the PTFE film moves toward the right from the position above copper-1 to that above copper-2 [Figure 2c-(v)]. The existence of the potential difference causes positive charge transfer between copper-1 and copper-2, thus causing a current to be generated in the external circuit. With continuous movement, the PTFE film moves to be entirely above copper-2, and the charge balance is then restored [Figure 2c-(vi)]. Because the device can be used for different excitation directions, the PTFE film can also move toward the left, and its

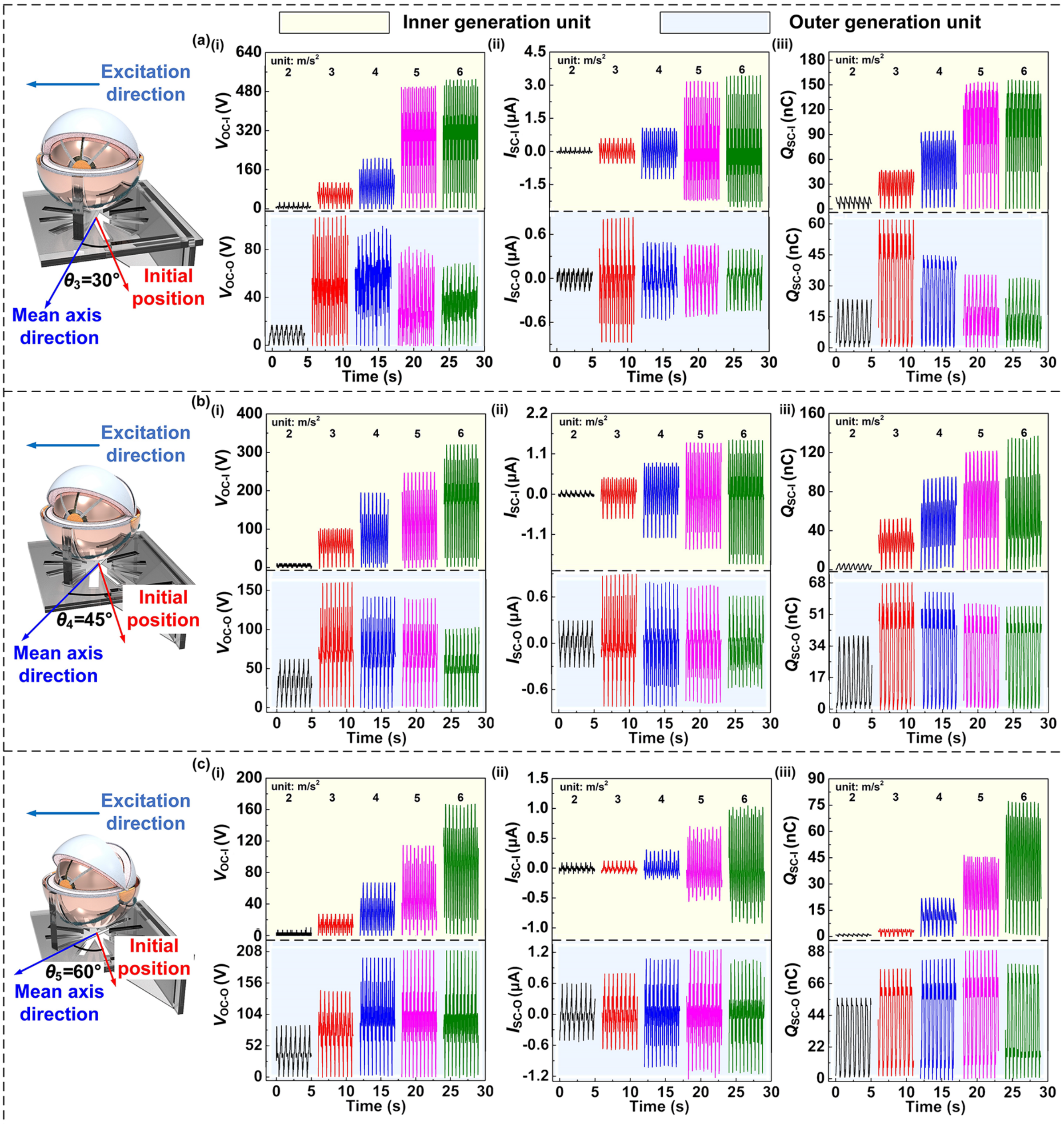

Figure 3. Output performances of the inner and outer generation units of the GS-TENG with an eccentric ball mass of 200 g under continuous excitation using different accelerations and different deflection angles: (a) 30°; (b) 45°; (c) 60°.

working principle remains the same. With continuous movement of the GS-TENG, the current can be generated continuously. To express the electron transfer process involved in this process more clearly, COMSOL Multiphysics 5.5 finite element simulation software was used to simulate and analyze the potential difference in different states (see Figure S3, Supporting Information).

Performance. To research the energy harvesting ability of the GS-TENG under excitation by waves propagating in different directions, a linear motor is used to simulate the wave motion to allow the device to operate normally. A specially made acrylic frame consisting of a support base, a bottom plate, and a motor connecting plate is installed on the linear motor. In the experiments, the GS-TENG is placed on a support base to receive the motor excitation, and the mean axis of the inner cage of the GS-TENG is horizontal to that of the support base. At the initial position, the excitation direction of the motor lies perpendicular to the mean axis direction of the inner cage; i.e., it lies horizontal to the mean axis direction of the outer cage. Different angle grooves are cut on the bottom plate, and the deflection angle relative to the initial position is varied by installing the support base on the different angle grooves. These different deflection angles lead to different excitation directions for the two generation units, thus verifying the energy harvesting capability of the GS-TENG in different directions. In this experiment, the movement distance for the motor is set at 50 mm, and the excitation acceleration of the motor is set at values of 2, 3, 4, 5, and 6 m/s^2. The deflection angle of the GS-TENG is then varied to study the output performances of the inner and

https://doi.org/10.1021/acsnano.2c01594
ACS Nano XXXX, XXX, XXX−XXX

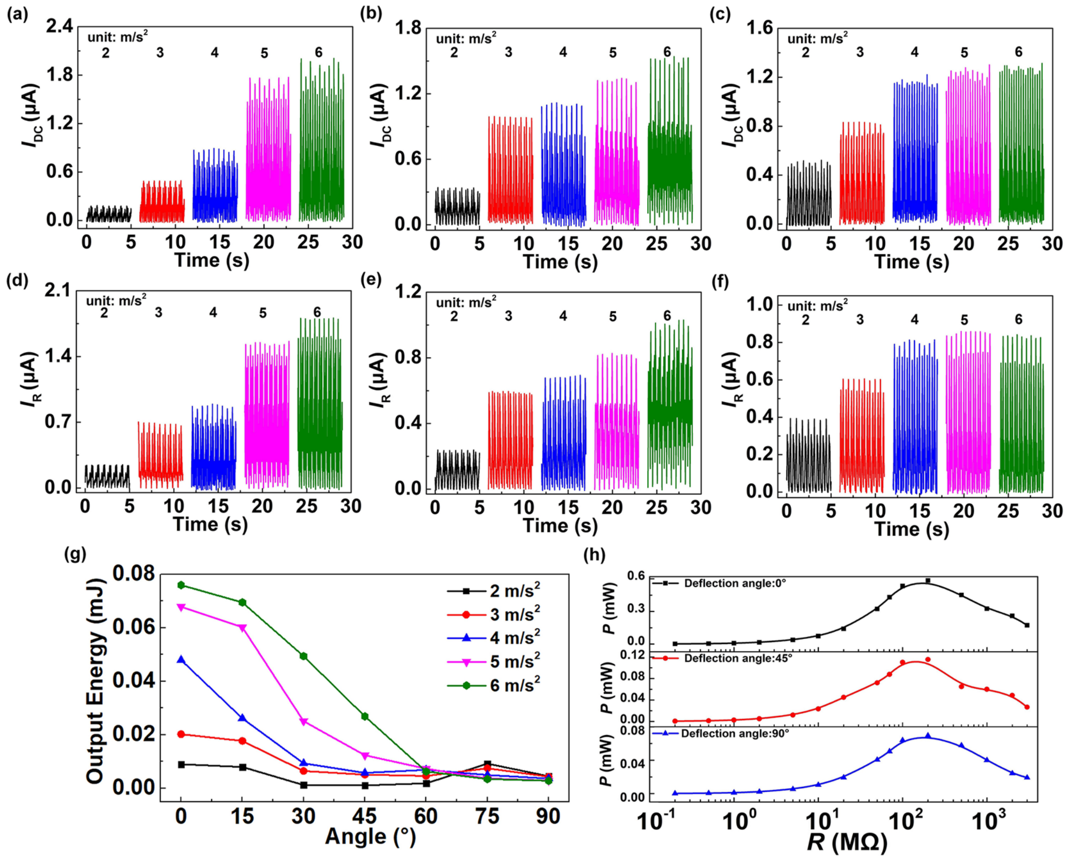

Figure 4. Direct-current and load-current output by two generation units of the GS-TENG connected in parallel under continuous excitation at different deflection angles and accelerations: (a), (d) 30°; (b), (e) 45°; (c), (f) 60°. (g) Output energy characteristics at different angles. (h) Peak power curves at three special deflection angles.

outer generation units. Seven different deflection angles are set in the experiment: 0°, 15°, 30°, 45°, 60°, 75°, and 90°.

The mass of the eccentric ball has a specific influence over the entire swing state, and thus at the initial position (where the deflection angle is 0°), the influence of different eccentric ball masses on the output performance of the GS-TENG is first studied (Figure S4, Supporting Information). The experiments show that the output performance is best when the mass of the eccentric ball is 200 g; in particular, at 6 m/s^2, the open-circuit voltage can reach 730 V, and the mass is thus set to have this value in subsequent experiments. Figure 3 panels a−c show comparisons of the open-circuit voltages, the short-circuit currents, and the transferred charges of the inner and outer generation units for deflection angles of 30°, 45°, and 60°, respectively. For the inner generation unit, under the same deflection angle condition, the output performance improves with increasing excitation acceleration; under the same acceleration, a smaller deflection angle provides better output performance. This occurs because the input excitation direction moves closer to the horizontal when the deflection angle increases, which means that the swing amplitude of the eccentric ball decreases.

In contrast, because the two generation units are oriented perpendicular to each other, the output performance of the outer generation unit improves when the deflection angle increases. The GS-TENG has a multilayer structure that causes the swing of the inner shell to be influenced by the swing of the eccentric ball to some extent. At different deflection angles, the inner shell will resonate with the eccentric ball at a specific acceleration, with the largest swing amplitude and the best output performance of the outer generation unit. The acceleration required to realize the resonance will also change when the deflection angle changes. However, because the inner shell itself has no counterweight, its swing amplitude is not as good as that of the eccentric ball, which causes the overall output performance of the outer generation unit to be weaker than that of the inner generation unit. At deflection angles of 15°, 75°, and 90°, the output performance varies while following the rule described above (Figure S5, Supporting Information). The design of the vertical axis means that only the outer generation unit can operate at 90°, and its open-circuit voltage can reach 160 V at 6 m/s^2. The experiments described above verify that the GS-TENG can harvest the input energy effectively from all directions.

To effectively study the overall output performance of the GS-TENG and facilitate the energy management in the subsequent real-wave environment, the two generation units are respectively connected in series with a rectifier bridge through an external circuit, and then output in parallel. Similarly, the output direct-current signals of the GS-TENG in seven different deflection directions are collected with the motor as excitation (Figure 4a−c and Figure S6a−d, Supporting Information). When the excitation acceleration increases, the peak value of the output direct current increases in tandem; however, when the deflection angle increases, the peak value then decreases. When the acceleration reaches 6 m/s^2 and the deflection angle is in the 0−90° range, the direct-current output by the GS-TENG can reach 0.8−3.2 μA. This occurs because the outer generation unit

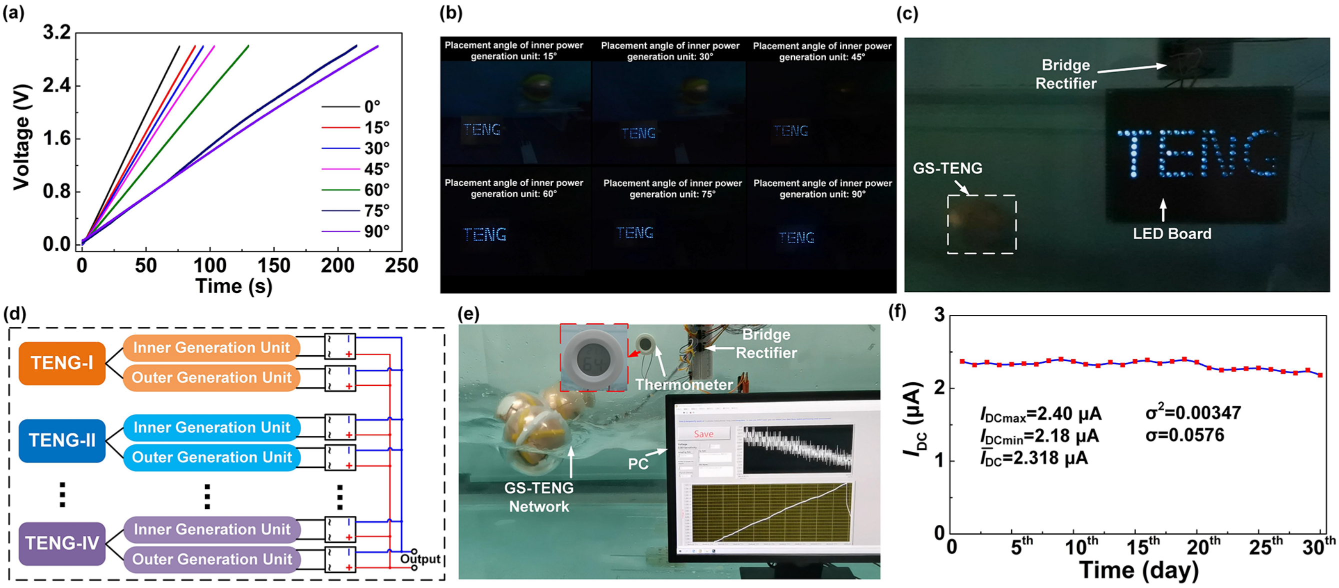

Figure 5. Use of a line motor to excite the GS-TENG in multiple directions to (a) charge a capacitor with a value of 10 μF and (b) light an LED board, where water waves were the excitation source. (c) LED board when lit by the GS-TENG. (d) Schematic TENG network diagram. (e) Thermometer energized by the GS-TENG network. (f) Results of a 1 month endurance experiment in the water.

gradually becomes the main output body, but the overall output performance of this unit is slightly weaker than that of the inner generation unit.

When the ambient resistor has a value of 200 MΩ, the change rule for the load current is the same (see Figure 4d−f and Figure S6e−h, Supporting Information). On the basis of this behavior, the relationship between the different deflection angles and the output energy under different excitation acceleration conditions was obtained (Figure 4g). Due to the influence of resonance, at a deflection angle of 75°, its performance is the best at 2 m/s^2, so it is different from other angles. In addition, at three special deflection angles (0°, 45°, 90°), the load currents were measured for different ambient resistors, and the corresponding peak power characteristics were then calculated (Figure 4h). At a deflection angle of 0°, the peak power of the GS-TENG can reach 0.6 mW, and its calculated power density is 0.28 W/m^3. The series of experiments described above verified that the GS-TENG has a multidirectional energy harvesting capability.

Demonstration. In addition to the basic performance of the GS-TENG, it is equally important to study the practical application capability of the device. With a linear motor as an excitation source and setting an acceleration of 6 m/s^2, the GS-TENG was used at different deflection angles to charge a 10 μF capacitor (Figure 5a). Similarly, under the same excitation conditions, the GS-TENG was able to light up an LED board successfully at any angle (Figure 5b, Video S1). The two experiments described above proved that the GS-TENG can operate normally under excitation in any direction.

Furthermore, to verify the applicability of the GS-TENG in a real-wave environment, a test bench was built with a linear motor and a large water tank to simulate a real-water-wave environment, and the GS-TENG was then placed in the water to allow it to move freely. The amplitude of the linear motor was set at 100 mm, and the acceleration was set at 5 m/s^2. Under excitation by the water waves, the GS-TENG illuminated the LED board continuously (Figure 5c, Video S2). To realize large-scale water wave energy harvesting, it is necessary to study the performance of several TENGs after they have been networked and connected. In this work, four identical GS-TENGs were networked, and the circuit connection mode was as shown in Figure 5d. In each GS-TENG, the inner generation unit and the outer generation unit were connected in series with a rectifier bridge to convert the AC output into a DC output. Subsequently, the complete parallel output was carried out of the circuit to avoid any mutual influence between the TENGs during free movement. With this connection, the TENG network successfully lit up a commercial thermometer via an external circuit in the water (Figure 5e, Video S3). Because the GS-TENG is used to harvest wave energy from water, it is necessary for the device to have good waterproofing and high stability. The output signal from a GS-TENG in water was collected within a fixed time period every day for 30 consecutive days (Figure 5f). After 30 days, the output DC current of the GS-TENG is reduced by about 8% compared with the initial one, and this underwater durability test proved the good stability and reliability of the device.

CONCLUSIONS

In summary, a GS-TENG has been designed in this work for application to multidirectional ocean wave energy harvesting. With reference to the gyroscope's structure, the GS-TENG has a structure composed of two cages with their central axes perpendicular to each other, thus enabling the two generation units in the GS-TENG to harvest wave energy from different directions effectively. Moreover, surface contact friction is adopted in the two generation units, which effectively increases the power generation area. The experimental test results prove that the GS-TENG has a multidirectional energy harvesting capability, and its output performance will vary according to the different excitation directions. Under continuous excitation by real waves, the GS-TENG illuminated an LED board continuously; additionally, several GS-TENG networks were able to drive a commercial thermometer. In particular, the GS-TENG showed good reliability that was verified by performing underwater experiments over 30 consecutive days. This research also provides concepts for the subsequent structural design of

https://doi.org/10.1021/acsnano.2c01594
ACS Nano XXXX, XXX, XXX−XXX

other TENGs and the realization of large-scale blue ocean energy development.

EXPERIMENTAL SECTION

Fabrication of the GS-TENG. The eccentric ball (Φ = 100 mm), inner shell (Φ = 120 mm), outer shell (Φ = 160 mm), and waterproof shell (Φ = 180 mm) in the gyroscope-structured triboelectric nanogenerator are all made of acrylic material. The counterweight materials in the eccentric ball and waterproof shell are sand. All cages and support seats are manufactured by 3D printing and made of polylactic acid (PLA). Eight copper electrodes (thickness 100 μm) are evenly distributed on the inner wall of the inner shell and the inner wall of the outer shell, respectively. A hole (width 5 mm and length 160 mm) is cut every 90° on the inner shell, for placing the same size rabbit fur strips, with the length of hair being about 40 mm. Set the same on the outer shell (the hole length is 205 mm). A sponge substrate (inner diameter 100 mm, outer diameter 112 mm, and length 140 mm) is arranged on the eccentric ball every 90°, and an equal PTFE film (thickness 0.08 mm) is pasted on it. The same arrangement is on the outer wall of the inner shell (inner diameter 120 mm, outer diameter 148 mm, and length 230 mm).

Electrical Measurement. The output signal of the GS-TENG is measured and collected by a programmable electrometer (6514, Keithley, USA) and a data acquisition system (PCI-6259, National Instruments, USA). External excitation is provided by a motor (PL01-19 × 600/520, LinMot, Switzerland), and it also makes water waves. LabVIEW records the collected signals.

ASSOCIATED CONTENT

Supporting Information

(MP4) The Supporting Information is available free of charge at https://pubs.acs.org/doi/10.1021/acsnano.2c01594.

Inner generation unit details; operation mechanism of the inner generation unit of the GS-TENG under excitement from different directions; simulations of the device in four states; under the continuous excitation of different accelerations and eccentric ball mass, the output performance of the inner generation unit of the GS-TENG when the deflection angle is 0°; under the continuous excitation of different accelerations and different deflection angles, the open-circuit voltage, short-circuit current, and transfer charge output by the inner and outer generation units of the GS-TENG with an eccentric ball mass of 200 g; output performance of the outer generation unit when the angle is at 90°; under continuous excitation, the direct-current and load-current output by two generation units of the GS-TENG in parallel at different deflection angles and different accelerations (PDF)

Lighting LED board by the GS-TENG under different deflection angles (MP4)

Lighting LED board by the GS-TENG under wave conditions (MP4)

Powering a thermometer by the GS-TENG network under wave conditions (MP4)

AUTHOR INFORMATION

Corresponding Authors

Tinghai Cheng − *Beijing Institute of Nanoenergy and Nanosystems, Chinese Academy of Sciences, Beijing 101400, China; School of Nanoscience and Technology, University of Chinese Academy of Sciences, Beijing 100049, China; CUSTech Institute of Technology, Wenzhou, Zhejiang 325024, China;* orcid.org/0000-0003-0335-7614; Email: chengtinghai@binn.cas.cn

Zhong Lin Wang − *Beijing Institute of Nanoenergy and Nanosystems, Chinese Academy of Sciences, Beijing 101400, China; School of Nanoscience and Technology, University of Chinese Academy of Sciences, Beijing 100049, China; CUSTech Institute of Technology, Wenzhou, Zhejiang 325024, China; School of Materials Science and Engineering, Georgia Institute of Technology, Atlanta, Georgia 30332-0245, United States;* orcid.org/0000-0002-5530-0380; Email: zhong.wang@mse.gatech.edu

Authors

Qi Gao − *Beijing Institute of Nanoenergy and Nanosystems, Chinese Academy of Sciences, Beijing 101400, China; School of Nanoscience and Technology, University of Chinese Academy of Sciences, Beijing 100049, China*

Yuhong Xu − *Beijing Institute of Nanoenergy and Nanosystems, Chinese Academy of Sciences, Beijing 101400, China*

Xin Yu − *Beijing Institute of Nanoenergy and Nanosystems, Chinese Academy of Sciences, Beijing 101400, China*

Zhaoxu Jing − *Beijing Institute of Nanoenergy and Nanosystems, Chinese Academy of Sciences, Beijing 101400, China*

Complete contact information is available at: https://pubs.acs.org/10.1021/acsnano.2c01594

Author Contributions

[⊥]Qi Gao and Yuhong Xu contributed equally to this work.

Notes

The authors declare no competing financial interest.

ACKNOWLEDGMENTS

The authors are grateful for the support received from the National Key R & D Project from Minister of Science and Technology (2021YFA1201601 and 2021YFA1201604), and the Beijing Natural Science Foundation (No. 3222023).

REFERENCES

(1) Wang, Z. L. Catch Wave Power in Floating Nets. *Nature* **2017**, *542*, 159−160.
(2) Wang, Z. L.; Song, J. Piezoelectric Nanogenerators Based on Zinc Oxide Nanowire Arrays. *Science* **2006**, *312*, 242−246.
(3) Wang, Z. L. Entropy Theory of Distributed Energy for Internet of Things. *Nano Energy* **2019**, *58*, 669−672.
(4) Wang, Z. L.; Jiang, T.; Xu, L. Toward the Blue Energy Dream by Triboelectric Nanogenerator Networks. *Nano Energy* **2017**, *39*, 9−23.
(5) Zhang, L.; Han, C.; Jiang, T.; Zhou, T.; Li, X.; Zhang, C.; Wang, Z. L. Multilayer Wavy-Structured Robust Triboelectric Nanogenerator for Harvesting Water Wave Energy. *Nano Energy* **2016**, *22*, 87−94.
(6) Fan, F.; Tian, Z.; Wang, Z. L. Flexible Triboelectric Generator. *Nano Energy* **2012**, *1*, 328−334.
(7) Wang, Z. L. Triboelectric Nanogenerators as New Energy Technology and Self-Powered Sensors-Principles, Problems and Perspectives. *Faraday Discuss.* **2014**, *176*, 447−458.
(8) Wang, Z. L. On Maxwell's Displacement Current for Energy and Sensors: The Origin of Nanogenerators. *Mater. Today* **2017**, *20*, 74−82.
(9) Wang, J.; Li, S.; Yi, F.; Zi, Y.; Lin, J.; Wang, X.; Xu, Y.; Wang, Z. L. Sustainably Powering Wearable Electronics Solely by Biomechanical Energy. *Nat. Commun.* **2016**, *7*, 12744.
(10) Wang, Z. L.; Wang, A. On the Origin of Contact-Electrification. *Mater. Today* **2019**, *30*, 34−51.
(11) Kim, B.; Chung, J.; Moon, H.; Kim, D.; Lee, S. Elastic Spiral Triboelectric Nanogenerator as a Self-Charging Case for Portable Electronics. *Nano Energy* **2018**, *50*, 133−139.
(12) Guo, H.; Wen, Z.; Zi, Y.; Yeh, M.; Wang, J.; Zhu, L.; Hu, C.; Wang, Z. L. A Water-Proof Triboelectric-Electromagnetic Hybrid

Generator for Energy Harvesting in Harsh Environments. *Adv. Energy Mater.* **2016**, *6*, 1501593.
(13) Zhong, W.; Xu, L.; Wang, H.; An, J.; Wang, Z. L. Tilting-Sensitive Triboelectric Nanogenerators for Energy Harvesting from Unstable/Fluctuating Surfaces. *Adv. Funct. Mater.* **2019**, *29*, 1905319.
(14) Wang, X.; Wen, Z.; Guo, H.; Wu, C.; He, X.; Lin, L.; Cao, X.; Wang, Z. L. Fully Packaged Blue Energy Harvester by Hybridizing a Rolling Triboelectric Nanogenerator and An Electromagnetic Generator. *ACS Nano* **2016**, *10*, 11369−11376.
(15) Kim, S.; Haines, C.; Li, N.; Kim, K.; Mun, T.; Choi, C.; Di, J.; Oh, Y.; Oviedo, J.; Bykova, J.; et al. Harvesting Electrical Energy from Carbon Nanotube Yarn Twist. *Science* **2017**, *357*, 773−778.
(16) Yang, W.; Wang, Y.; Li, Y.; Wang, J.; Cheng, T.; Wang, Z. L. Integrated Flywheel and Spiral Spring Triboelectric Nanogenerator for Improving Energy Harvesting of Intermittent Excitations/Triggering. *Nano Energy* **2019**, *66*, 104104.
(17) Wang, Y.; Yu, X.; Yin, M.; Wang, J.; Gao, Q.; Yu, Y.; Cheng, T.; Wang, Z. L. Gravity Triboelectric Nanogenerator for the Steady Harvesting of Natural Wind Energy. *Nano Energy* **2021**, *82*, 105740.
(18) Li, A.; Zi, Y.; Guo, H.; Wang, Z. L.; Fernández, F. Triboelectric Nanogenerators for Sensitive Nano-Coulomb Molecular Mass Spectrometry. *Nat. Nanotechnol.* **2017**, *12*, 481−487.
(19) Liu, S.; Li, X.; Wang, Y.; Yang, Y.; Meng, L.; Cheng, T.; Wang, Z. L. Magnetic Switch Structured Triboelectric Nanogenerator for Continuous and Regular Harvesting of Wind Energy. *Nano Energy* **2021**, *83*, 105851.
(20) Lin, H.; Liu, Y.; Chen, S.; Xu, Q.; Wang, S.; Hu, T.; Pan, P.; Wang, Y.; Zhang, Y.; Li, N.; Li, Y.; Ma, Y.; Xie, Y.; Wang, L. Seesaw Structured Triboelectric Nanogenerator with Enhanced Output Performance and Its Applications in Self-Powered Motion Sensing. *Nano Energy* **2019**, *65*, 103944.
(21) Chung, J.; Yong, H.; Moon, H.; Duong, Q.; Choi, S.; Kim, D.; Lee, S. Hand-Driven Gyroscopic Hybrid Nanogenerator for Recharging Portable Devices. *Adv. Sci.* **2018**, *5*, 1801054.
(22) Wang, Z.; Yu, Y.; Wang, Y.; Lu, X.; Cheng, T.; Bao, G.; Wang, Z. L. Magnetic Flap Type Difunctional Sensor for Detecting Pneumatic Flow and Liquid Level Based on Triboelectric Nanogenerator. *ACS Nano* **2020**, *14*, 5981−5987.
(23) Xu, Q.; Lu, Y.; Zhao, S.; Hu, N.; Jiang, Y.; Li, H.; Wang, Y.; Gao, H.; Li, Y.; Yuan, M.; Chu, L.; Li, J.; Xie, Y. A Wind Vector Detecting System Based on Triboelectric and Photoelectric Sensors for Simultaneously Monitoring Wind Speed and Direction. *Nano Energy* **2021**, *89*, 106382.
(24) Xu, Q.; Fang, Y.; Jing, Q.; Hu, N.; Lin, K.; Pan, Y.; Xue, L.; Gao, H.; Ming, Y.; Chu, L.; Ma, Y.; Xie, Y.; Chen, J.; Wang, L. A Portable Triboelectric Spirometer for Wireless Pulmonary Function Monitoring. *Biosens. Bioelectron.* **2021**, *187*, 113329.
(25) Shi, Q.; Wu, H.; Wang, H.; Wu, H.; Lee, C. Self-Powered Gyroscope Ball Using a Triboelectric Mechanism. *Adv. Energy Mater.* **2017**, *7*, 1701300.
(26) Guo, H.; Chen, J.; Wang, L.; Wang, A.; Li, Y.; An, C.; He, J.; Hu, C.; Hsiao, V.; Wang, Z. L. A Highly Efficient Triboelectric Negative Air Ion Generator. *Nat. Sustain* **2021**, *4*, 147−153.
(27) Lei, R.; Shi, Y.; Ding, Y.; Nie, J.; Li, S.; Wang, F.; Zhai, H.; Chen, X.; Wang, Z. L. Sustainable High-Voltage Source Based on Triboelectric Nanogenerator with a Charge Accumulation Strategy. *Energy Environ. Sci.* **2020**, *13*, 2178−2190.
(28) Wang, Z. L. Triboelectric Nanogenerator (TENG)-Sparking an Energy and Sensor Revolution. *Adv. Energy Mater.* **2020**, *10*, 2000137.
(29) Khan, U.; Kim, S. Triboelectric Nanogenerators for Blue Energy Harvesting. *ACS Nano* **2016**, *10*, 6429−6432.
(30) Chen, H.; Xing, C.; Li, Y.; Wang, J.; Xu, Y. Triboelectric Nanogenerators for a Macro-Scale Blue Energy Harvesting and Self-Powered Marine Environmental Monitoring System. *Sustain. Energy Fuels* **2020**, *4*, 1063−1077.
(31) Wang, Y.; Liu, X.; Chen, T.; Wang, H.; Zhu, C.; Yu, H.; Song, L.; Pan, X.; Mi, J.; Lee, C.; Xu, M. An Underwater Flag-Like Triboelectric Nanogenerator for Harvesting Ocean Current Energy Under Extremely Low Velocity Condition. *Nano Energy* **2021**, *90*, 106503.
(32) Rodrigues, C.; Nunes, D.; Clemente, D.; Mathias, N.; Correia, J.; Rosa-Santos, P.; Taveira-Pinto, F.; Morais, T.; Pereira, A.; Ventura, J. Emerging Triboelectric Nanogenerators for Ocean Wave Energy Harvesting: State of the Art and Future Perspectives. *Energy Environ. Sci.* **2020**, *13*, 2657−2683.
(33) Liang, X.; Jiang, T.; Feng, Y.; Lu, P.; An, J.; Wang, Z. L. Triboelectric Nanogenerator Network Integrated with Charge Excitation Circuit for Effective Water Wave Energy Harvesting. *Adv. Energy Mater.* **2020**, *10*, 2002123.
(34) Liu, W.; Xu, L.; Liu, G.; Yang, H.; Bu, T.; Fu, X.; Xu, S.; Fang, C.; Zhang, C. Network Topology Optimization of Triboelectric Nanogenerators for Effectively Harvesting Ocean Wave Energy. *iScience* **2020**, *23*, 101848.
(35) Zhong, W.; Xu, L.; Yang, X.; Tang, W.; Shao, J.; Chen, B.; Wang, Z. L. Open-Book-Like Triboelectric Nanogenerators Based on Low-Frequency Roll-Swing Oscillators for Wave Energy Harvesting. *Nanoscale* **2019**, *11*, 7199−7208.
(36) Wang, A.; Chen, J.; Wang, L.; Han, J.; Su, W.; Li, A.; Liu, P.; Duan, L.; Xu, C.; Zeng, Z. Numerical Analysis and Experimental Study of an Ocean Wave Tetrahedral Triboelectric Nanogenerator. *Appl. Energy* **2022**, *307*, 118174.
(37) Yin, M.; Lu, X.; Qiao, G.; Xu, Y.; Wang, Y.; Cheng, T.; Wang, Z. L. Mechanical Regulation Triboelectric Nanogenerator with Controllable Output Performance for Random Energy Harvesting. *Adv. Energy Mater.* **2020**, *10*, 2000627.
(38) Gao, W.; Shao, J.; Sagoe-Crentsil, K.; Duan, W. Investigation on Energy Efficiency of Rolling Triboelectric Nanogenerator Using Cylinder-Cylindrical Shell Dynamic Model. *Nano Energy* **2021**, *80*, 105583.
(39) Yuan, Z.; Wang, C.; Xi, J.; Han, X.; Li, J.; Han, S.; Gao, W.; Pan, C. Spherical Triboelectric Nanogenerator with Dense Point Contacts for Harvesting Multidirectional Water Wave and Vibration Energy. *ACS Energy Lett.* **2021**, *6*, 2809−2816.
(40) Feng, Y.; Liang, X.; An, J.; Jiang, T.; Wang, Z. L. Soft-Contact Cylindrical Triboelectric-Electromagnetic Hybrid Nanogenerator Based on Swing Structure for Ultra-Low Frequency Water Wave Energy Harvesting. *Nano Energy* **2021**, *81*, 105625.
(41) Davies, D. Charge Generation on Dielectric Surfaces. *J. Phys. D: Appl. Phys.* **1969**, *2*, 1533.